Research

Recrystallization and Sulfur Diffusion in $CdCl_2$-Treated CdTe/CdS Thin Films

B.E. McCandless,* L.V. Moulton† and R.W. Birkmire
Institute of Energy Conversion, University of Delaware, Newark, DE 19716-3820, USA

The role of $CdCl_2$ in prompting recrystallization, grain growth and interdiffusion between CdS and CdTe layers in physical vapor-deposited CdS/CdTe thin-film solar cells is presented. Several CdTe/CdS thin-film samples with different CdTe film thicknesses were treated in air at 415°C for different times with and without a surface coating of $CdCl_2$. The samples were characterized by scanning electron microscopy, transmission electron microscopy, energy dispersive x-ray spectroscopy, x-ray diffractometry and optical absorption. The results show that $CdCl_2$ treatment enhances the recrystallization and diffusion processes, leading to a compositional variation within the CdTe layer due to diffusion of sulfur from the CdS. The highest sulfur concentrations observed after 30 min treatments with $CdCl_2$ at 415°C are near the solubility limit for sulfur in CdTe. The compositional distributions indicated by x-ray diffraction measurements of samples with different CdTe thickness show that the S-rich $CdTe_{1-x}S_x$ region lies near the CdTe/CdS interface. A multiple-step mixing process must be inferred to account for the diffraction profiles obtained.

Prog. Photovolt. Res. Appl., **5**, 249–260 (1997)

No. of Figures: 7. No. of Tables: 2. No. of References: 22.

INTRODUCTION

Post-deposition processing of polycrystalline CdS/CdTe solar cells with $CdCl_2$ has been demonstrated to improve cell efficiency by improving the electrical properties of the films for photovoltaic operation.[1] In many cases the treatment also produces significant structural changes that are coupled to the electronic properties of the semiconducting layers and can impose limits on device performance. Treatment or exposure to $CdCl_2$ is a component of every process for fabricating high-efficiency CdTe solar cells, regardless of CdTe film formation temperature. For example, films that are fabricated from sintered powder slurries are processed with $CdCl_2$ additives at temperatures of 600–700°C to encourage grain growth and film densification.[2–5] Other devices, such as those deposited by physical vapor deposition (PVD) and molecular beam epitaxy, receive a lower temperature treatment to achieve efficiencies in the 11–13% range.[6,7] They are coated with a $CdCl_2 : CH_3OH$ solution, dried, then heat treated at ~400°C. Cells formed by electrochemical deposition receive an analogous treatment where they are synthesized in a

* Correspondence to: B. E. McCandless, Institute of Energy Conversion, University of Delaware, Newark, DE 19716-3820, USA
† Current address: 22 Sandhill Road, Morristown, NJ 07960, USA

Contract grant sponsor: National Renewable Energy Laboratory; Contract grant number: XAV-3-13170-01

CCC 1062–7995/97/040249–12$17.50

Received 3 March 1997
Revised 23 May 1997

plating bath containing Cl ions to produce a Cl-doped CdTe layer and then heat treated at 400°C for 30 min.[8]

Many effects of the $CdCl_2$ processing on the CdTe/CdS layers have been observed but their significance to device operation have not been quantitatively explained. For example, grain growth in both the CdS and CdTe layers is greatly enhanced, while porosity is minimized,[1–8] but among the different high-efficiency devices represented, a considerable range of grain size, porosity and film orientation is found. Previous work has also established that substantial sulfur diffusion occurs in CdTe films over a wide range of thermal processing temperatures.[2–6] A significant degree of sulfur diffusion has also been noted following 400°C treatments with $CdCl_2$ in which consistent shifts were observed in the CdTe x-ray diffraction spectra, CdTe optical absorption edge, and the CdTe spectral response cut-off in CdS/CdTe solar cells.[1,6,9] In addition, secondary ion mass spectroscopy (SIMS) has shown that the average sulfur content of the CdTe film increases as the distance to the CdS/CdTe interface decreases (A. Nelson and S. Asher, NREL, pers. comm.). During high-temperature treatments ($T > 500$°C) sulfur diffusion into CdTe is believed to have led to homojunction formation within the S-rich portion of the $CdTe_{1-x}S_x$ layer.[4,5] These observations are all consistent with the diffusive transport of sulfur into CdTe during $CdCl_2$ processing, which reduces the CdS window layer and forms a $CdTe_{1-x}S_x$ layer. Likewise, Te diffusion into CdS produces $CdS_{1-y}Te_y$, which reduces the high-energy portion of the device spectral response, resulting in lower current densities. Recrystallization treatments of the CdS layer have been developed that limit the extent of this process.[10,11] The extent of the CdS consumption establishes a lower limit to the thickness of CdS that can be employed to achieve high efficiency. Control over the effective CdS thickness obtained after processing is thus critical to achieving high current densities while retaining the junction properties of the CdTe/CdS, which controls the open-circuit voltage of the device. Loss of the CdS layer will result in the formation of a $CdTe_{1-x}S_x$/TCO junction having inferior performance.[10]

This paper examines recrystallization and sulfur diffusion in CdTe at ~400°C through a detailed analysis of CdTe/CdS structures before and after the $CdCl_2$ treatment as a function of treatment time. The treatment temperature and time range used in this work were selected to be in the range used to make high-efficiency devices. Macroscopic and microscopic materials analyses were performed to assess changes in structure and composition of the CdTe layer.

EXPERIMENTAL

Film deposition and $CdCl_2$ treatment

The CdS/CdTe cells were prepared in a superstate configuration, so that light enters the cell through the transparent conductive oxide (TCO)-coated glass superstrate. First, 0.2–0.5 μm of CdS was deposited at 200°C by evaporation onto indium tin oxide (ITO)-coated 7059 glass substrates. Then CdTe films of several thicknesses (0.5, 1, 2 and 4 μm) were evaporated at a growth rate of ~8 Å s^{-1} and a substrate temperature of 250°C on top of the CdS layers. These deposition conditions yielded uniform single-phase CdTe films. For transmission electron microscopy (TEM), samples with 2 μm of CdTe on 0.5 μm of CdS were deposited on polished Si wafers coated with ITO. To ensure that the CdTe/CdS deposited on this substrate yielded comparable electrical performance to the standard cells, a semi-transparent Au layer was used as the contact to CdTe to allow backwall current–voltage measurements to be made. Comparable backwall performance was obtained from the two device structures.

The CdTe/CdS/ITO/7059 samples were coated with 0.8 μm of solid $CdCl_2$ by placing one drop per cubic centimeter of 1 wt% $CdCl_2$–CH_3OH solution on the top surface of the CdTe film and then evaporating the CH_3OH in a drying oven at 85°C. During the subsequent hot air treatment the samples were held at 415°C for either 10 or 30 min. Thermal transients were minimized by rapid introduction and withdrawal of the samples from the hot zone of the furnace tube. The heat treatment step was followed by a rinse in deionized water to remove most of the residual $CdCl_2$ coating.

Microscopy measurements

The CdTe grain sizes were determined using the method of Heyn[12] from the top surface of the CdTe film and from polished 90° sample cross-sections using scanning electron microscopy (SEM). The CdTe grains were clearly distinguishable on the top surface of the samples once they had been rinsed. Polished and etched 90°C cross-sections were prepared by vacuum impregnation in epoxy, polishing with 0.05-μm alumina grit and then rinsing in hot water.

The CdTe grain boundaries in the polished samples were revealed by first etching in a 0.0125 wt% $Br_2 : CH_3OH$ solution and then reacting in a 0.1 M CuCl–deionized water solution (adjusted to pH 2.25 by the addition of HC) at 65°C for 30–60 s. The reaction $CdTe + 2CuCl \rightarrow CdCl_2 + Cu_2Te$ occurs preferentially along grain boundaries. To reveal the grain boundaries, the $Cu_{2-x}Te$ was etched in a 0.2 M KCN–water solution at 65°C for 30 s. After each step, the samples were rinsed with room temperature, deionized water and dried.

Transmission electron microscopy (TEM) and energy-dispersive x-ray spectroscopy (EDS) were used to examine the cross-sectional grain structure and composition on a CdTe/CdS/ITO/Si sample before and after heat treatment with $CdCl_2$.[13]

X-ray diffraction measurements

The x-ray diffraction (XRD) patterns of the CdTe films were generated using a computer-controlled Philips/Norelco diffractometer with Bragg-Bretano focusing geometry and Cu K_α radiation. Wide-angle 2θ scans from 20–80° taken at 0.05° steps were used to identify the phases present in the samples. The Rachinger correction[14] was used to remove α_2 components for lattice parameter determination and peak profile examination. Errors in peak centrum location associated with specimen placement and geometry were corrected using the function of Nelson, Riley, Sinclair and Taylor (NRST), so that the CdTe film lattice parameters could be determined precisely.[15–17] The sulfur content, x, of the $CdTe_{1-x}S_x$ film was determined quantitatively from the lattice parameters by assuming a Vegard's relation

$$x = 1.508(6.481 - a) \tag{1}$$

where a is the lattice parameter of the sample. The error in lattice parameter determination was typically ± 0.001 Å, translating to an error in sulfur content of $\pm 0.2\%$.

The degree of preferred orientation in the films was calculated from the α_1 peak intensities of the broad scans using the method of Harris for polycrystalline fiber texture analysis.[18] For the {111} reflection, the orientation parameter, $p(111)$, is defined

$$p(111) = N\left[\frac{I(111)}{I_0(111)}\right] \cdot \left[\sum \frac{I(hkl)}{I_0(hkl)}\right]^{-1} \tag{2}$$

where N is the number of peaks in the region considered, I(hkl) is the measured intensity of peak (hkl) and $I_0(hkl)$ is the relative intensity of the corresponding peak from a powder reference. For $p(111) = N$, all the grains of the films are oriented in the ⟨111⟩ direction normal to the substrate, while $p(111) = 1$ indicates random grain orientation and $p(111) < 1$ indicates preferred orientation along an axis other than ⟨111⟩.

Diffraction scans at 0.01° steps were acquired at constant counts per step to obtain a constant signal-to-noise ratio from sample to sample for individual peak profile determination. The peak profiles were assumed to represent the entire sample alloy composition range resulting from diffusion of sulfur into CdTe. The diffractometer angular resolution permits compositional resolution of 0.1 mol.%. To ensure the validity of this assumption, primary and diffracted beam attenuation, which increases surface selectivity, was minimized by using samples < 3 μm thick. One film was mechanically separated from the TCO/glass and remeasured from the CdS side, yielding the same diffraction profile. To obtain adequate angular resolution, higher order peaks such as the (422), (511) and the (531) were measured. The extent of sulfur diffusion into the grains was shown to be independent of the grain orientation with respect to the

substrate surface by examining all (hkl) peak profiles on a single sample. Profiles exhibiting high symmetry, and therefore low diffusion tails, were fitted to a Pearson VII function[19] to determine the full width at half-maximum (FWHM) for comparison with the diffractometer instrument function. In cases of high asymmetry, Fourier deconvolution of the diffractometer instrument function was performed to establish the limits of compositional broadening.

Optical absorption measurements

Optical transmission, $T(\lambda)$, and reflection, $R(\lambda)$, of the CdTe/CdS/ITO/glass structures were measured on a Perkin-Elmer Lambda 9 spectrophotometer and were transformed to an effective absorption coefficient, $\alpha_e(\lambda)$, to allow comparison of the absorption edge location after the various treatments. For this, the effective absorption coefficient of the structure was determined by

$$\alpha_e(\lambda) = \frac{1}{d} \ln\left[\frac{T(\lambda)}{1 - R(\lambda)}\right] \tag{3}$$

where d is the thickness. Plots of α_e^2 versus energy were used to determine relative shifts in the absorption edge due to the alloying of CdTe and CdS over a sufficient film thickness to influence the overall absorption. The sulfur content of the absorbing layer was estimated by comparison of the shift of the absorption edge with that reported for kinetically limited or metastable $CdTe_{1-x}S_x$ thin films[20,21] in which the CdTe bandgap, E_g, is reduced due to bowing of the $E_g(x)$ curve with a minimum at $x \sim 25\%$

$$E_g(x) = 1.74x^2 - 1.01x + 1.51 \tag{4}$$

Equilibration of alloy films at ~400°C leads to a miscibility gap from $x = 5.8\%$ to $x = 97\%$ but with similar E_g versus x dependence over the alloy existence region.

RESULTS

Microscopy

As-deposited films have a lateral grain size of ~0.1–0.25μm, depending on film thickness. Films heat treated 415°C without $CdCl_2$ for up to 30 min have a similar structure to as-deposited films, with little observable change in grain size or morphology. However, substantial grain growth occurs for samples coated with $CdCl_2$. Figure 1 shows SEM top surface micrographs of 0.5-, 1-, 2- and 4-μm thick CdTe films for as-deposited (Figure 1(a)–(c)) and $CdCl_2$ treated at 415°C for 10 min (Figure 1(d)–(f)) and 30 min (Figure 1(g)–(i)). For the different CdTe film thicknesses there is a trend toward large final grain sizes with thicker CdTe films and with longer heat treatment times, although for the 2-μm thick films, the average grain size is the same after 10 and 3 min of treatment (Table 1). After 30 min of treatment there are no detectable submicron grains and the grain boundaries meet at 120° angles, as expected for a film in equilibrium.[22]

Cross-section SEM micrographs in conjunction with top surface micrographs show that the increase in grain dimension extends down to the CdTe/CdS interface, as shown in Figure 2. Figure 2 demonstrates that the coalesced CdTe grains after $CdCl_2$ heat treatment are at least as wide as they are deep. This is quite different from the as-deposited microstructures, which are difficult to analyze by SEM analysis because the grain sizes are <250 nm.

Cross-section TEM analysis was carried out on as-deposited 2-μm CdTe/0.5 μm CdS samples and the same samples after $CdCl_2$ treatment at 415°C for 30 min. The micrographs of the CdTe/CdS/ITO/Si cross-sections suggest that the as-deposited CdTe grains are epitaxial with the underlying CdS grains and are highly faulted and columnar (Figure 3(a)). Spot TEM/EDS analysis showed no evidence of S or Te interdiffusion in the as-deposited films. Selected area electron diffraction of the individual layers showed

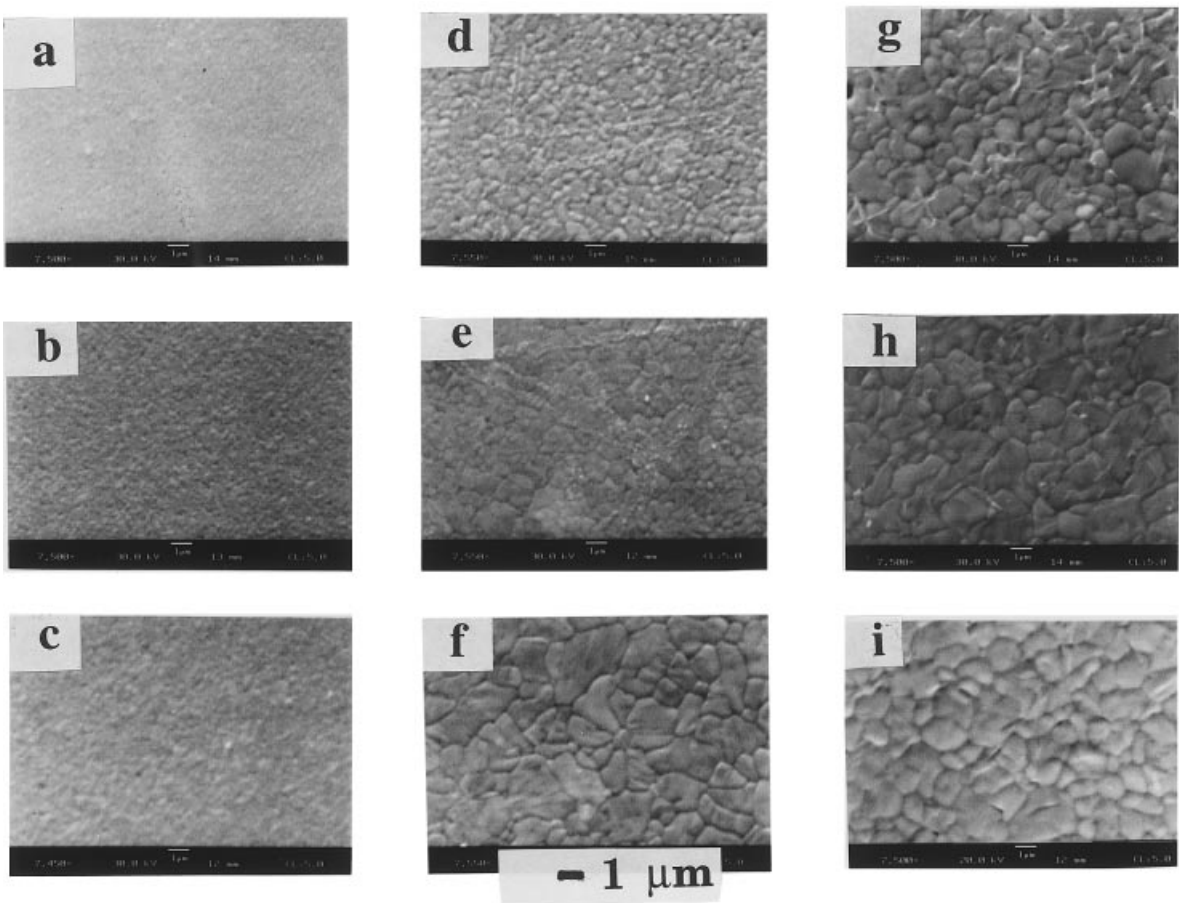

Figure 1. Top surface SEM micrographs of 0.5-, 1- and 2-μm CdTe/0.5-μm CdS/ITO/glass structure in as-deposited condition (a–c); after heat treatment at 415°C for 10 min with $CdCl_2$ (d–f); and after heat treatment at 415°C for 30 min with $CdCl_2$ (g–i)

that the CdTe film is predominantly cubic, while the CdS film contains a mixture of cubic and hexagonal phases. High-resolution lattice imaging confirmed that the CdTe grains are epitaxially related to the CdS grains.[13] After heat treatment with $CdCl_2$, TEM imaging (Figure 3(b)) shows substantial grain growth in both layers with little or no epitaxial coordination between the CdS and the CdTe. The TEM micrographs show thermal grooving at the surface of the CdTe near the grain boundaries and independent

Table I. Tabulated values of grain size, orientation parameter, lattice parameter and (111) peak intensity for CdTe powder and for CdTe films in 2-μm CdTe/0.5-μm CdS/ITO/glass structures

Sample	Condition[a]	Average grain size (μm)	p(111)	I(111) (counts)	a_0 (Å)	(511) FWHM (degrees)
Powder	—	NA[b]	1.0	NA	6.481	NA
Film	As-deposited	0.2	4.0	8849	6.489	0.248
Film	10 and 30 min HT and no $CdCl_2$	0.2	2.3	4908	6.480	0.140
Film	10 min HT with $CdCl_2$	1.3	0.8	5823	6.481	0.140
Film	30 min HT with $CdCl_2$	1.3	0.9	3004	6.460	>0.40

[a]HT = heat treatment
[b] = not applicable

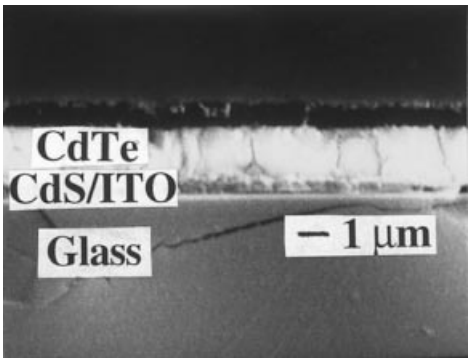

Figure 2. Cross-section SEM micrograph of 2-μm thick CdTe sample after heat treatment at 415°C for 30 min with $CdCl_2$

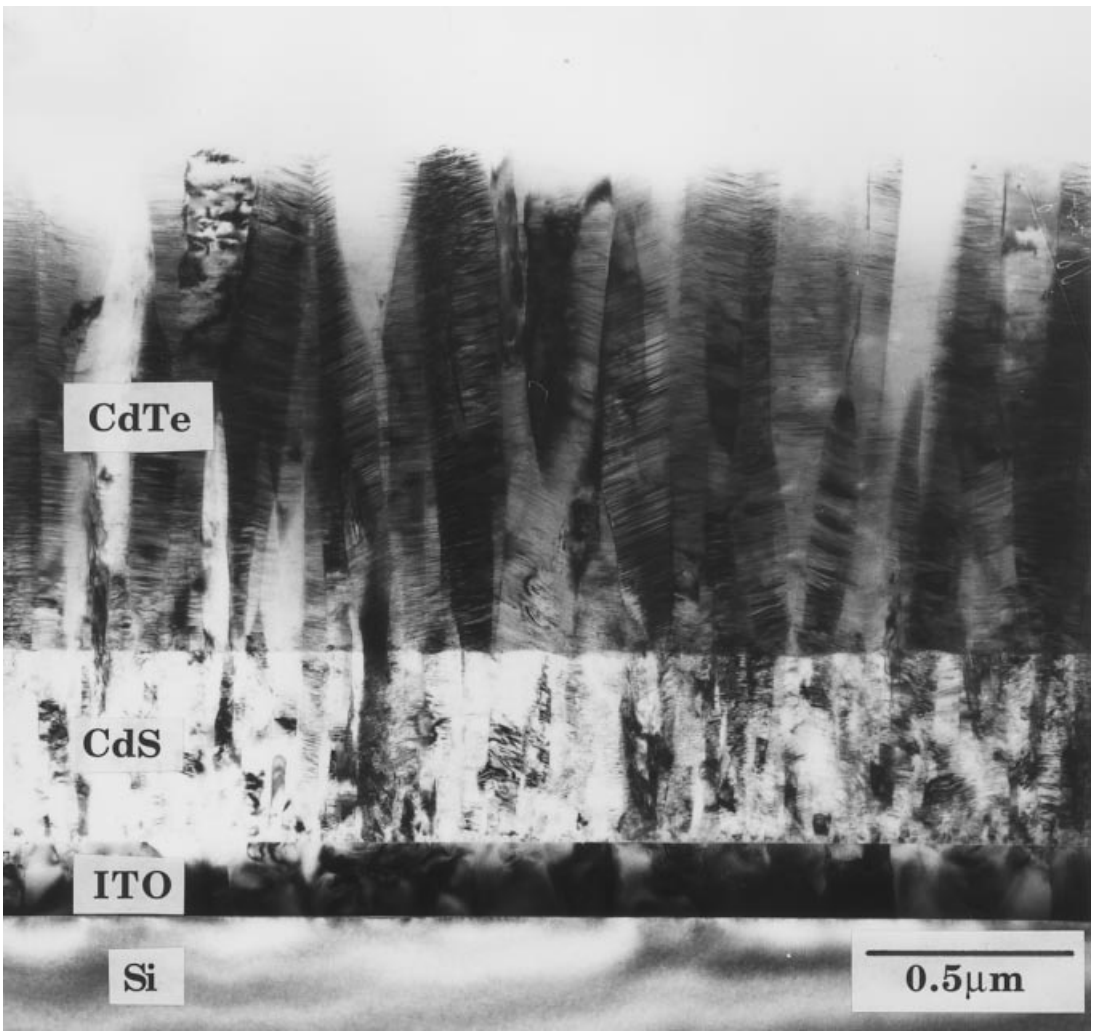

Figure 3. (a) (*Continued opposite*)

restructuring of the CdS and CdTe films, resulting from reduction in the interfacial energy. Selected-area EDS measurements indicated S and Te interdiffusion across the interface after treatment.

Wide-angle x-ray diffraction scans

Wide-angle x-ray diffraction scans were made on all samples: as-deposited, treated without $CdCl_2$ and treated with $CdCl_2$ at 415°C for 10 and 30 min. The XRD scans show that recrystallization of the CdTe film occurs during heat treatment with or without $CdCl_2$. Figure 4 specifically compares an as-deposited sample to treated samples cut from the same piece. The treatments were performed for 10 and 30 min with $CdCl_2$ and for 10 min without $CdCl_2$. The as-deposited film shows a very strong {111} texture with $p(111) = 4$. Heat treatment at 415°C for 10 or 30 min in the absence of $CdCl_2$ produces a modest degree of sharpening of the individual peaks and a reduction of preferred orientation to $p(111) = 2.3$. Heat treatment of $CdCl_2$-coated samples at 415°C for 10 min, however, produces near-random orientation of

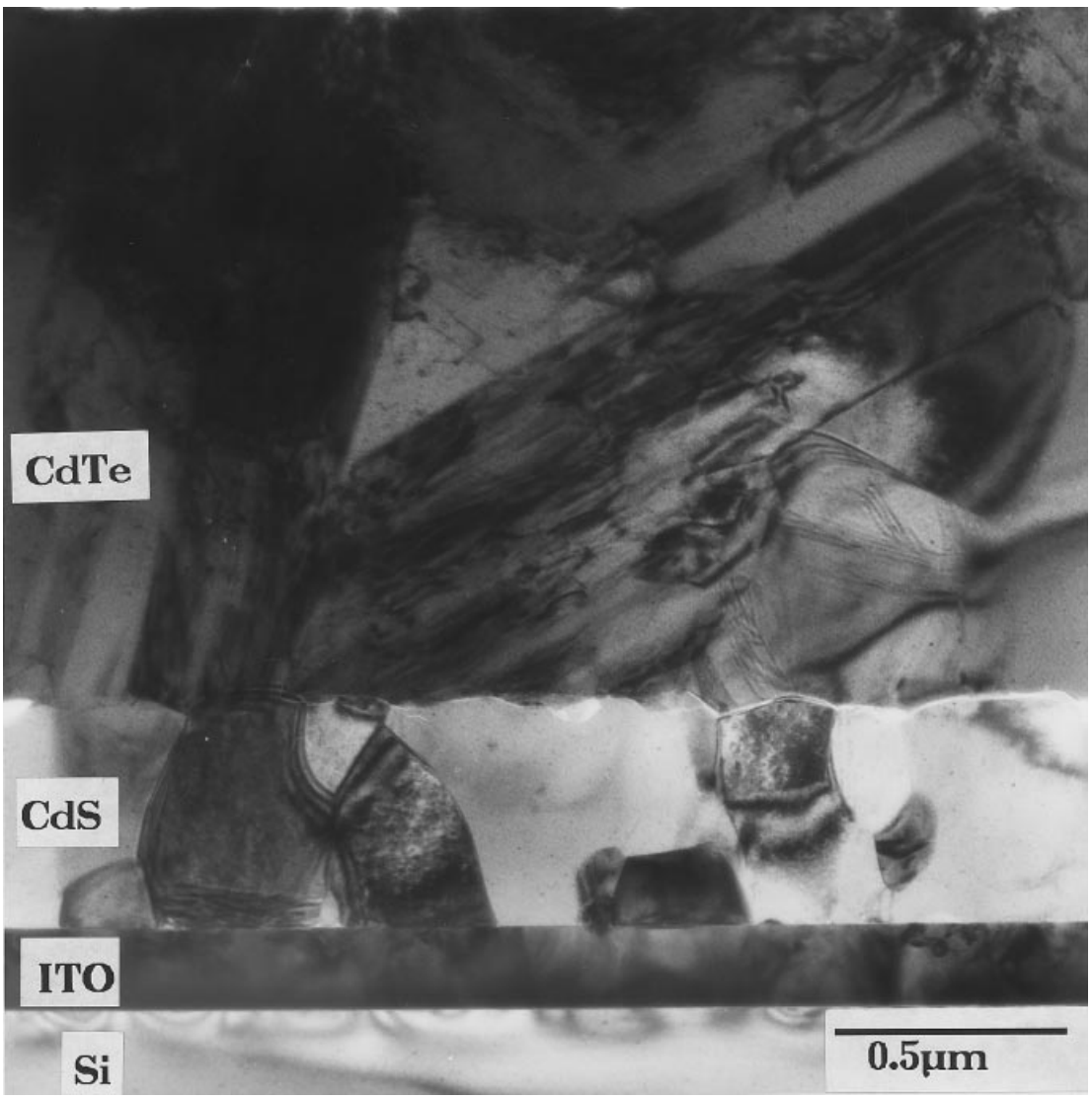

Figure 3. Cross-section transmission electron micrograph of 2-μm CdTe/0.5-μm CdS/ITO/Si in as-deposited condition (a) and after heat treatment at 415°C for 30 min with $CdCl_2$ (b)

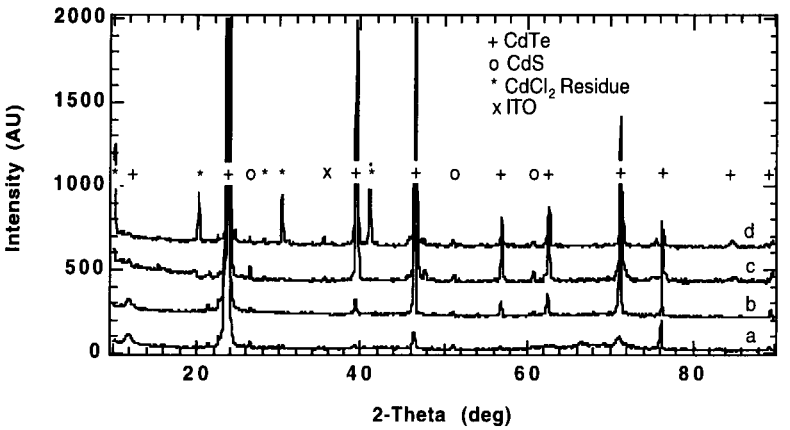

Figure 4. Wide-angle XRD scans of 2-μm CdTe/0.5-μm CdS/ITO/glass structure in as-deposited condition (a), after heat treatment at 415°C for 10 min with no $CdCl_2$ (b), after heat treatment at 415°C for 10 min with $CdCl_2$ (c) and after heat treatment at 415°C for 30 min with $CdCl_2$

the grains, with $p(111) < 2$. The samples treated with $CdCl_2$ also exhibit additional peaks in the patterns due to residual $CdCl_2$ phases on the CdTe surface after treatment.

Heat treatment without $CdCl_2$ shifted all the diffraction peaks slightly towards a higher angle, while treatment $CdCl_2$ shifted and broadened the diffraction peaks towards a higher angle. Table I summarizes the changes in grain size, orientation parameter, precision lattice parameter and FWHM obtained with and without $CdCl_2$ during heat treatment. The as-deposited films appear to be slightly strained, with a lattice parameter of 0.13% that was greater than expected for CdTe. This increase in a_0 along the $\langle hkl \rangle$ growth axis can be explained by a compressive stress perpendicular to the growth axis, i.e. in the growth plane. The TEM results described above suggest that the hetero-epitaxial nature of the CdTe/CdS films can account for the residual strain in the as-deposited films, given the ~10% lattice mismatch between atoms in the CdS (001) and CdTe (111) planes , although other sources of strain such as impurities cannot be ruled out. Heat treatment without $CdCl_2$ relieves the strain, which produces the observed reorientation and shift in a_0 to that expected for pure CdTe. Consistent with prior work,[5,8] the heat treatment with $CdCl_2$ shifts the centrum of the CdTe peaks towards a smaller lattice parameter. This is explained by the diffusion of sulfur into CdTe to form a $CdTe_{1-x}S_x$ solid solution, because sulfur substitutes onto Te sites in the CdTe lattice and has a smaller atomic radius than Te, which thus reduces the interatomic bond length in the molecule.

Narrow-angle x-ray diffraction scans

High-resolution scans of all (*hkl*) diffraction lines show the same profile, indicating that the CdS/CdTe mixing process is independent of crystallographic direction. Analysis of the (511) CdTe diffraction peaks before and after $CdCl_2$ processing was made to illustrate the strain relief and compositional variations promoted by the $CdCl_2$ processing. Figure 5 shows the (511) peak profile of 1-μm thick CdTe film in the as-deposited state and after 10- and 30-min $CdCl_2$ heat treatments at 415°C. The evolution of the profile indicates either a strain state and/or compositional inhomogeneity in the CdTe film. Our subsequent analysis is based on the latter assumption, given the supporting evidence of the TEM/EDS and SIMS measurements.

In Figure 5, the centrum of the as-deposited (511) peak profile again has larger *d*-spacing than expected for pure, unstrained CdTe. The FWHM of the (511) peak is approximately twice that of the diffractometer instrument function. After 10 and 30 min of treatment with $CdCl_2$ and 10 min with $CdCl_2$ the peak shifted to the *d*-spacing expected for pure CdTe and sharpened to the value obtained for the diffractometer instrument function. Increasing the heat treatment time to 60 min without $CdCl_2$ resulted in the

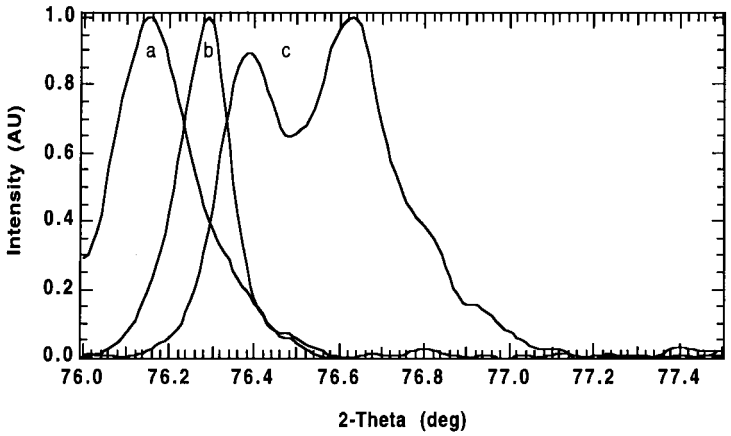

Figure 5. The XRD (511) profile of 2-μm CdTe/0.5-μm CdS/ITO/glass structure in as-deposited condition (a), after heat treatment at 415°C for 10 min with $CdCl_2$ (b) and after heat treatment at 415°C for 30 min with $CdCl_2$ (c)

same *d*-spacing as obtained after 10 and 30 min. Grain coalescence reduced small-particle scattering and relieved the strain, resulting in a sharper peak profile and a lattice parameter shift. After 30 min of treatment with $CdCl_2$ the peak profile is a doublet with a significant tail extending towards lower *d*-spacing and lattice parameter.

Fourier deconvolution of the diffractometer instrument function from this profile indicates two strong maxima centered at $a_0 = 6.478$ Å and $a_0 = 6.459$ Å, corresponding to compositions of $x = 0.5\%$ and $x = 3.3\%$, respectively in $CdTe_{1-x}S_x$. The high-angle tail extends to the solubility limit found for sulfur in CdTe.[21] Chemical removal of the top micron of film eliminated the high-a_0 component of the diffraction profile so that the low-sulfur portion of the film was removed. Thus, the S-enriched portion lies in the region of the structure closest to the CdS/CdTe interface. The resulting profile is similar to the profiles obtained from thinner CdTe samples treated under exactly the same conditions, as presented in Figure 6. This implies that a compositional distribution with depth is obtained that is independent of the total CdTe thickness and suggests a rapid diffusion process near the CdS/CdTe interface. Thus, treatment with $CdCl_2$ results in CdS/CdTe mixing that cannot be accounted for by a simple single-step diffusion process. In curves (b) and (c) of Figure 6, for 1.0-μm and 0.5-μm thick CdTe films, the primary peak has shifted to the lower lattice parameter, indicating conversion of most of the film to $CdTe_{1-x}S_x$, with

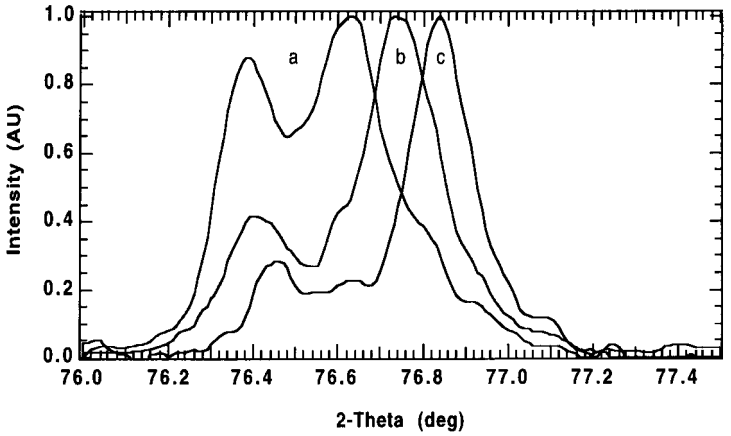

Figure 6. The XRD (511) profile after heat treatment at 415°C for 30 min with $CdCl_2$ of 2-μm CdTe/0.5-μm CdS/ITO/glass structure (a), 1-μm CdTe/0.5-μm CdS/ITO/glass structure (b), and 0.5-μm CdTe/0.5-μm CdS/ITO/glass structure (c)

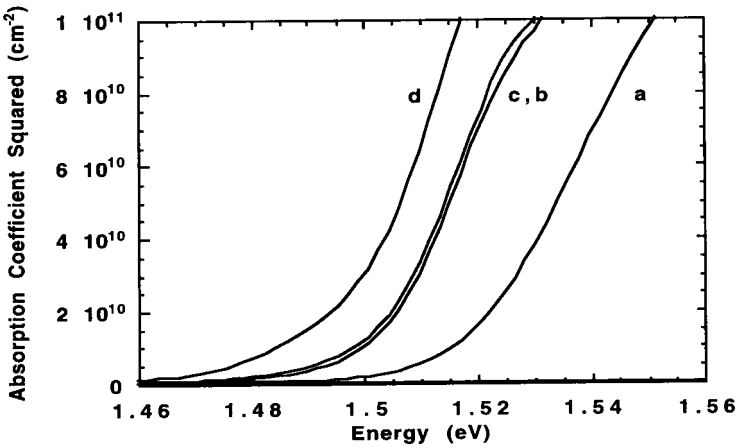

Figure 7. Absorption coefficient squared versus energy for 2-μm CdTe/0.5-μm CdS/ITO/glass structure in as-deposited condition (a), after heat treatment at 415°C for 10 min with no $CdCl_2$ (b), heat treatment at 415°C for 10 min with $CdCl_2$ (c) and heat treatment at 415°C for 30 min with $CdCl_2$ (d)

$x = \sim 5\%$. In a 1-μm CdTe film, this corresponds to an equivalent CdS film thickness of ~40 nm that is consumed during the processing.

Optical absorption measurements

A plot of the square of the absorption coefficient versus photon energy is shown in Figure 7 for the 2-μm CdTe/0.5-μm CdS samples of Table I. All samples exhibit similar absorption profiles, and the energy shifts caused by the different treatments are listed in Table II.

Table II. Tabulated values of relative energy shifts from the as-deposited film at $\alpha^2 = 5 \times 10^{10}$ cm^{-2} in Figure 7 and the corresponding sulfur content

Sample	Condition[a]	ΔE (meV)	% S
a	As-deposited	0	0
b	10, 30 and 60 min HT and no $CdCl_2$	19	1.95
c	10 min HT with $CdCl_2$	20	2.05
d	30 min HT with $CdCl_2$	28	2.95

[a]HT = heat treatment

The samples treated for 10, 30 and 60 min without $CdCl_2$ and for 10 min with $CdCl_2$ exhibited the same reductions in the energy of the absorption edge with the formation of a $CdTe_{1-X}S_X$ layer containing ~2% S. After treatment for 30 min with $CdCl_2$, however, the composition of the lowest-bandgap absorbing layer corresponds to $CdTe_{1-x}S_x$ containing ~3% S. At first glance, these compositions do not seem to be supported by the diffraction data, but the diffraction data are least sensitive to thin layers near the interface, while the optical data are most sensitive to highly absorbing layers of low bandgap, as expected near the interface. Thus, in the region of the interface, treatment at 400°C with or without $CdCl_2$ produces some intermixing of CdTe and CdS. This mixing is the primary mechanism for relieving elastic strain in as-deposited samples. For the sample treated with $CdCl_2$ for 30 min, the optical measurements indicate the presence of a layer with 3% S, while the diffraction data consistently exhibit a maximum at ~3% but tails that extend to 5–6% S, at the solubility limit for sulfur in CdTe.[22] It is speculated that the higher sulfur content regions do not form a continuous film of sufficient thickness to control the optical

properties in the plane parallel to the interface. Thus, the higher sulfur content regions (3–6% S) may exist along grain boundaries or other defects.

CONCLUSIONS

As-deposited evaporated CdTe/CdS thin-film structures consist of single-phase columnar CdTe grains that are pseudo-epitaxially oriented on mixed cubic and hexagonal phase CdS films. The CdTe film is highly strained due to lattice mismatch and is free of sulfur.

Heat treatment of the structures at 415°C without $CdCl_2$ produces little or no detectable grain growth but relaxes interfacial strain due to a small amount of interfacial CdTe/CdS mixing. The treatment also induces some randomization of the CdTe film orientation with respect to the ⟨111⟩ axis.

Heat treatment with $CdCl_2$, needed to produce high-efficiency devices from the evaporated materials, induces dramatic grain growth of both the CdTe and CdS layers, reduces surface and interfacial energy, promotes significant CdS/CdTe interdiffusion and randomizes the CdTe film orientation. The recrystallization occurs in a time frame of ~10 min at 415°C, while interdiffusion is progressive up to 30 min and may involve more than one transport process to account for the doublet diffraction peak profiles observed. Further work is necessary to identify the mixing processes and their dependence on $CdCl_2$ concentration, reaction temperature and treatment time. The region near the original CdS/CdTe interface consists of a $CdTe_{1-x}S_x$ alloy with $x \approx 5\%$, which is the equilibrium solubility limit for sulfur in CdTe. The extensive alloying forms a non-uniform $CdTe_{1-x}S_x$ layer and consumes a significant quantity of CdS from the device. This establishes a lower limit to the CdS film thickness that can be employed while still retaining a discrete CdS coating on the TCO.

Acknowledgements

The authors wish to acknowledge the technical contributions of Herbert Wardell and Michael Goetz of the Institute of Energy Conversion and Mowafak M. Al-Jassim and Sally Asher of the National Renewable Energy Laboratory. The Authors also thank John D. Meakin and Matheswaran Marudachalam for useful discussions. This work was supported by the National Renewable Energy Laboratory under subcontract no. XAV-3-13170-01.

REFERENCES

1. B. E. McCandless and R. W. Birkmire, *Sol. Cells*, **31**, 527 (1991).
2. I. Clemminck, M. Burgelman, M. Casteleyn, J. Depoorter and A. Vervaet, *Proc. 22nd IEEE PVSC*, Las Vegas, 1991, p. 1114.
3. H. Matsumoto, A. Nakano, H. Uda, S. Ikegami and T. Miyazawa, *Jpn. J. Appl. Phys.*, **21**, 800 (1982).
4. J. S. Lee, H. B. Kim, A. L. Fahrenbruch and R. H. Bube, *J. Electrochem. Soc.*, **134**, 1790 (1987).
5. J. S. Roh and H. B. Im, *J. Mater. Sci.*, **23**, 2267 (1988).
6. R. W. Birkmire, B. E. McCandless and S. S. Hegedus, *Int. J. Sol. Energy*, **12**, 145 (1992).
7. S. A. Ringle, A. W. Smith, M. H. MacDougal and A. Rohatgi, *J. Appl. Phys.*, **70**, 881 (1991).
8. S. K. Das and G. C. Morris, *Sol. Energy Mater. Sol. Cells*, **28**, 305 (1993).
9. D. G. Jensen, B. E. McCandless and R. W. Birkmire, *Proc. 25th IEEE PVSC*, Crystal City, 1996, p. 773–776.
10. B. E. McCandless and S. S. Hegedus, *Proc. 22nd IEEE PVSC*, 1991, pp. 967–972.
11. R. W. Birkmire, S. S. Hegedus, B. E. McCandless, J. E. Phillips, T. W. F. Russell, W. N. Shafarman, S. Verma and S. Yamanaka, *AIP Conf. Proc.*, **268**, 212 (1992).
12. S. H. Avner, *Introduction to Physical Metallurgy*, pp. 102–104, McGraw-Hill, New York, 1974.
13. M. M. Al-Jassim, F. S. Hasoon, K. M. Jones, B. M. Keyes, R. J. Matson and H. R. Moutinho, *Proc. 23rd IEEE PVSC*, 1993, p. 459.
14. W. A. Rachinger, J. Sci. Inst. **25**, 254 (1948)

15. C. Barrett and T. B. Massalski, *Structure of Metals*, 3rd Edn, p. 144, Pergamon Press, London, 1980
16. J. B. Nelson and D. P. Riley, *Proc. Phys. Soc.*, **57**, 160 (1945).
17. A. Taylor and H. Sinclair, *Proc. Phys. Soc.*, **57**, 126 (1945).
18. G. B. Harris, *Philos. Mag.*, **43**, 133 (1952).
19. R. A. Young and D. B. Wiles, *J. Appl. Cryst.*, **15**, 430–438 (1982).
20. K. Ohata, J. Saraie and T. Tanaka, *Jpn. J. Appl. Phys.*, **12**, 1641 (1973).
21. D. G. Jensen, B. E. McCandless and R. W. Birkmire, *Proc. 1996 MRS* Meeting, San Francisco, p. 325–336.
22. J. H. Brophy, R. M. Rose and J. Wulff, *Thermodynamics of Structure*, pp. 54–55. Wiley, New York, 1966.

